17th UK Conference on Computational Mechanics (ACME-UK)
6th–8th April 2009
Nottingham

Modelling Elasto-plasticity with the Hybrid Meshless Scaled Boundary Method

*** Claire E. Heaney[1] and Charles E. Augarde[2]**

[1] Durham University
School of Engineering
South Road
Durham DH1 3LE, UK
claire.heaney@durham.ac.uk
www.dur.ac.uk/claire.heaney

[2] Durham University
School of Engineering
South Road
Durham DH1 3LE, UK
charles.augarde@durham.ac.uk
www.dur.ac.uk/charles.augarde

Key Words: *Meshless or Meshfree Methods, Meshless Local Petrov-Galerkin, Scaled Boundary Method, Elasto-Plasticity.*

ABSTRACT

1 Introduction

Meshless methods have become a popular tool for dealing with problems that exhibit large deformations because no remeshing is required and also, extra nodes can be included relatively easily and in an unstructured arrangement. Despite these advantages, there are some fundamental difficulties with meshless methods such as imposing essential boundary conditions, the coupling together of domains and the effect of nodal arrangements on the quality of the solution. This paper presents evidence of some of these difficulties.

Many geotechnical problems involve both nonlinear constitutive models and unbounded domains. In order to design an efficient solution procedure, the domain can be split into two regions which will each model different aspects of the problem. The hybrid meshless scaled boundary method [1], does exactly this by coupling the meshless local Petrov-Galerkin (MLPG) method in the near-field to model material nonlinearities, with the scaled boundary method in the far-field to model linear elastic behaviour.

2 Governing equations

A typical problem is shown in figure 1, which can be thought of as a flexible strip footing (plane strain) on a half-space subject to a vertical, uniform load. This example is used for illustrative purposes, but the hybrid method is applicable to general elasto-static problems in 3D. Deeks and Augarde [1] consider the two regions seen in figure 1 separately, and construct equations which satisfy equilibrium and which couple together the two regions.

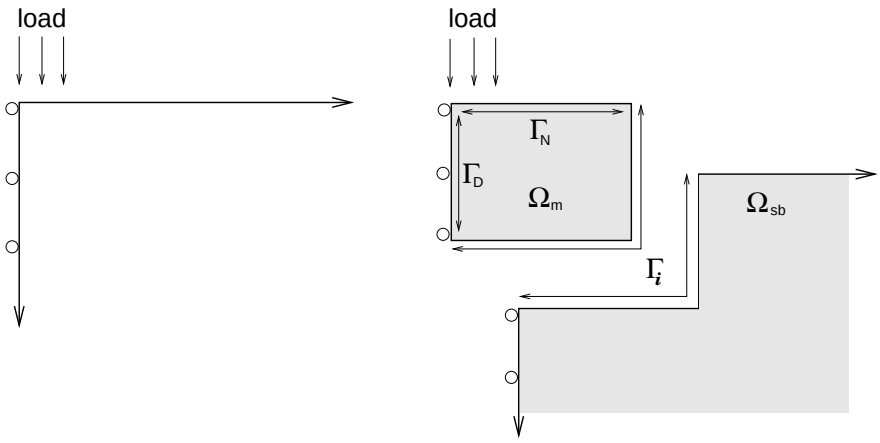

Figure 1: Left: the physical domain. Symmetry means that only half of the physical domain needs to be modelled where an appropriate boundary condition is applied along the line of symmetry. Right: the domain split into two, a meshless region, Ω_m and a scaled-boundary region, Ω_{sb}. The interface between these regions is given by Γ_i with the Dirichlet (Γ_D) and Neumann (Γ_N) boundaries indicated for the meshless region.

The interested reader may consult Deeks and Augarde [1,2] to see how the two domains are coupled together and how the governing equations are assembled. The result is given here. In the meshless region cartesian co-ordinates are used and the trial and test functions are given by $[N^1(x,y)]$ and $[N^2(x,y)]$ respectively. Derivatives of the trial and test functions are collected in the matrices $[B^1(x,y)]$ and $[B^2(x,y)]$. In the scaled-boundary region a radial co-ordinate ξ and circumferential co-ordinate s are used. The trial and test functions are given by $[N^1(s)]$, and $[N^2(s)]$, and the stiffness matrix is given by $[K_{sb}]$. The constitutive matrix is represented by $[D]$, and the independent components of the stress tensor are listed in a vector $\{\sigma\}$. The radial dependence is found by solving an eigenvalue problem. In the meshless domain, collecting the usual stiffness matrix, the traction across the interface and the compatibility condition for displacement (two terms), the problem to be solved is

$$\left(\int_{\Omega_m} [B^2(x,y)]^{\mathrm{T}}[D][B^1(x,y)]\, d\Omega_m - \int_{\Gamma_i} [N^2(x,y)]^{\mathrm{T}}[T][D][B^1(x,y)]\, d\Gamma_i \right.$$
$$\left. + \alpha \int_{\Gamma_i} [N^2(x,y)]^{\mathrm{T}}[N^1(x,y)]\, d\Gamma_i \right) \{\hat{u}_m\} - \alpha \int_{\Gamma_i} [N^2(x,y)]^{\mathrm{T}}[N^1(s)]\, d\Gamma_i \, \{u_{sb}\} = \{f_m\} \,. \quad (1)$$

A similar result can be found for the scaled-boundary domain, collecting the stiffness matrix, traction across the interface and compatibility

$$\left([K_{sb}] + \alpha \int_{\Gamma_i} [N^2(s)]^{\mathrm{T}}[N^1(s)] d\Gamma_i \right) \{u_{sb}\} + \left(\int_{\Gamma_i} [N^2(s)]^{\mathrm{T}} \left([T][D][B^1(x,y)] - \alpha [N^1(x,y)] \right) d\Gamma_i \right) \{\hat{u}_m\} = \{f_{sb}\} \,. \quad (2)$$

The shape functions $[N^1]$ are determined by a moving weighted least squares (MLS) approximation. In the MLPG method, as described in [3], each node has a region of compact support within which it affects the approximation. A weight function, associated with each node, determines how the nodal value affects the approximation at points within the region of support. Spline weight functions are used, so for the ith node the weight function is given by

$$w_i(x,y) = \begin{cases} 1 - 6\left(\dfrac{d}{r_i}\right)^2 + 8\left(\dfrac{d}{r_i}\right)^3 - 3\left(\dfrac{d}{r_i}\right)^4 & \text{for } 0 \leqslant d \leqslant r_i \\ 0 & \text{for } d > r_i \,, \end{cases}$$

where $d = \sqrt{(x - x_i)^2 + (y - y_i)^2}$. This information is fed into the MLS formulation and the shape functions are retrieved, for details see Atluri and Zhu [3]. The radius must be large enough so that there are enough nodes in support of each integration point to solve for necessary coefficients, but small enough so that the approximation will not be 'over-smooth'. Test functions $[N^2]$ are also required. In MLPG methods, these are usually taken to be the spline weight functions, only with a smaller radius than before. This makes the integration (which occurs over regions enclosed by the test radii) more efficient. The governing equations are solved on a region which comprises the union of all the test domains, so the test domains should cover the domain of the problem.

3 Results

The hybrid meshless scaled boundary method has been extended to include a nonlinear solution algorithm for material nonlinearities. A Newton-Raphson scheme is used to apply the load increments and the Prandtl-Reuss constitutive equation is solved with the Closest Point Projection scheme. At the initial stages of elasto-plastic behaviour the method produces results, however, before the ultimate bearing capacity is reached the scheme fails to converge. Figure 2 shows a plot of force applied to a flexible footing, against the surface displacement at the centre of the footing. Were more load applied, the curve would eventually flatten off signifying that the ultimate bearing capacity had been reached. As can be seen, the solution procedure cannot reach this stage. One possible explanation for this is that the coverage of the domain by the radii of the test functions is not complete. Another explanation is that the coupling of the two domains introduces inaccuracies in the solution in the vicinity of the interface, which will affect the solution throughout the domain. Evidence supporting the latter point has been seen in linear elastic simulations, which show higher than expected stress values close to the interface between the meshless and scaled boundary regions.

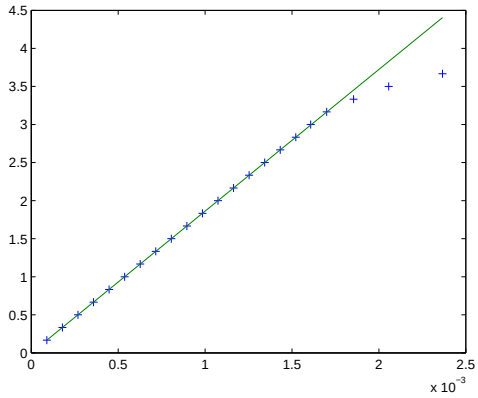

Figure 2: Load Displacement plot for a von Mises material.

Using just the meshless domain to solve footing problems allows us to investigate the affect of adjusting the nodal arrangement on the solution. Here, an elastic material is assumed for simplicity, and the meshless results are compared with a Finite Element solution. The five different nodal arrangements used can be seen in figure 3. The flexible footing problem was solved with these nodal arrangements and also on similar grids with higher nodal densities. Assuming the finite element solution to be accurate, we can see from figure 4 that the uniform grid performs by far the worst. The grid with staggered nodes under the footing is the next worse. The other three (irregular) grids perform similarly well.

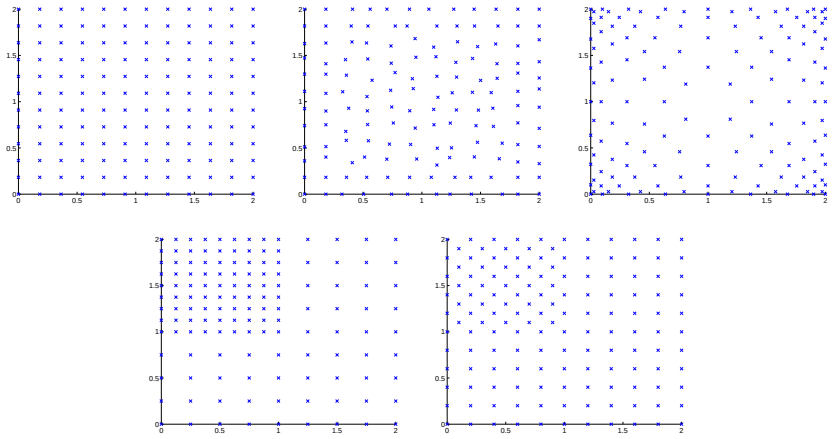

Figure 3: Nodal arrangements. Top row: left, a uniform grid ; centre, a randomly perturbed grid ; right, nodes based on Legendre Gauss-Lobatto (LGL) points (all 3 grids, 144 nodes each); bottom row: grids with extra nodes underneath the footing, in-line (left, 137 nodes) and staggered (right, 146 nodes).

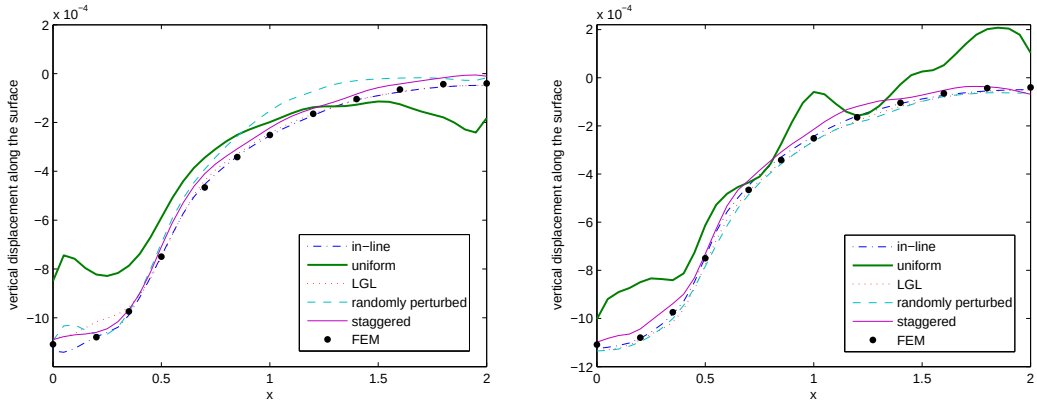

Figure 4: Plots of the surface displacement against horizontal distance x for a flexible footing on an elastic material ($E = 1000$MPa, $\nu = 0.25$), for approximately 140 nodes (left) and 400 nodes (right).

4 Conclusion

The coupling of the MLPG scaled boundary method and a 2D MLPG method needs further investigation before it can be used to model elasto-plastic material behaviour. For elastic simulations using only a (truncated) 2D meshless domain, uniform nodal arrangements produce inaccurate and oscillatory solutions when compared to non-uniform arrangements.

REFERENCES

[1] A. J. Deeks and C. E. Augarde. A hybrid meshless local Petrov-Galerkin method for unbounded domains. *Comp. Meth. Appl. Mech. Eng.*, 196:843–852, 2007.

[2] A. J. Deeks and C. E. Augarde. A meshless local Petrov-Galerkin scaled boundary method. *Computational Mechanics*, 36:159–170, 2005.

[3] S. N. Atluri and T. Zhu. A new Meshless Local Petrov-Galerkin (MLPG) approach in computational mechanics. *Computational Mechanics*, 22:117–127, 1998.